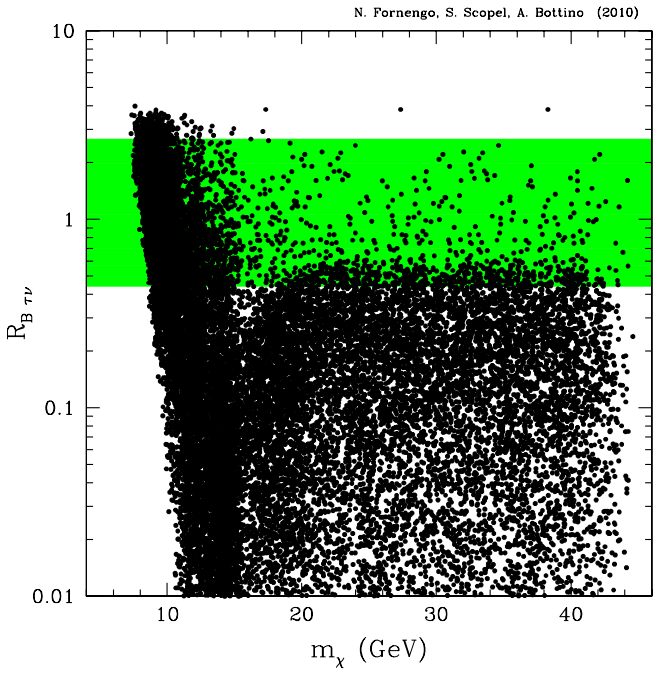


FIG. 17 (color online). Scatter plot of the quantity $R_{B\tau\nu}$, calculated according to Eqs. (37) and (38), as a function of $m_\chi$ in the LNM-$\mathcal{A}$ scan. The green horizontal band represents the range of Eq. (41).

of $\tan\beta$ and of $m_\chi$, respectively. These figures show that the present range of $R_{B\tau\nu}$ favors large values of $\tan\beta$ and would not have any impact on the lower bound of 7.5 GeV previously established.

As for the semileptonic decays $B \to D + l + \nu$, it is convenient to consider the ratio $R(D) \equiv BR(B \to D\tau\nu)/BR(B \to De\nu)$, since in this ratio many experimental systematic uncertainties cancel, either partially or completely [75]. Also some theoretical uncertainties cancel out in this ratio [76].

An experimental determination for $R(D)$ is provided by the *BABAR* Collaboration: $R(D) = (41.6 \pm 11.7(\text{stat}) \pm 5.2(\text{syst})) \times 10^{-2}$ [75]. A determination by the Belle Collaboration is given in the report of Ref. [77]: $R(D) = (60 \pm 14(\text{stat}) \pm 8(\text{syst})) \times 10^{-2}$. However, this value has been obtained by using the Belle determination $BR(B^+ \to \bar{D}^0\tau^+\nu) = (1.51^{+0.41}_{-0.39}(\text{stat})^{+0.24}_{-19}(\text{syst}) \pm 0.15) \times 10^{-2}$, which has recently been superseded by the new Belle determination $BR(B^+ \to \bar{D}^0\tau^+\nu) = (0.77 \pm 0.22(\text{stat}) \pm 0.12(\text{syst})) \times 10^{-2}$ [78], smaller than the previous one by a factor of 2. In view of the lack of an updated value for $R(D)$ provided by the Belle Collaboration and of the ambiguities which may rise in treating the uncertainties in the various branching ratios concurring in the determination of $R(D)$, in our discussion we only take into account the *BABAR* value previously mentioned. Notice however that the new Belle value for the branching ration of $B^+ \to \bar{D}^0\tau^+\nu$ approaches now considerably the *BABAR* value for the branching ratio of the process $B^+ \to \bar{D}^0\tau^+\nu$ [75].

From the *BABAR* determination $R(D) = (41.6 \pm 11.7(\text{stat}) \pm 5.2(\text{syst})) \times 10^{-2}$, we obtain the 95% C.L. range

$$13.5 \times 10^{-2} \leq R(D) \leq 69.7 \times 10^{-2}. \quad (42)$$

Figures 18 and 19 display the scatter plot for the quantity $R(D)$ evaluated by using the Eq. (9) of Ref. [76], versus $\tan\beta$ and $m_\chi$, respectively. We see that the experimental range of $R(D)$ given in Eq. (42) is compatible with the light-neutralino configurations.

In Fig. 20 we display $R_{B\tau\nu}$ and $R(D)$ as functions of the quantity $C^\tau_{NP}$ defined in Eq. (38). The curve with the parabolic shape represents $R_{B\tau\nu}$ as given by Eq. (37) and the almost straight line gives $R(D)$, calculated with Eq. (9) of Ref. [76]. The parts colored in red pertain to neutralino configurations with $m_\chi \leq 10$ GeV.

Notice that, should the indication of Fig. 20 be taken strictly, one would deduce for the quantity $C^\tau_{NP}$ two ranges of compatibility: $-0.51 \lesssim C^\tau_{NP} \lesssim -0.32$ and $-0.041 \lesssim C^\tau_{NP} \lesssim -0.065$. From this, by using Eq. (38), one finds that the range at large $\tan\beta$ for the quantity $\tan\beta/(m_{H^\pm}/120\ \text{GeV})$ is $30 \lesssim \tan\beta/(m_{H^\pm}/120\ \text{GeV}) \lesssim 40$.

This in turn would have some impact on the features of the neutralino population which substantially contribute to the DM abundance [i.e., for which $(\Omega_{\text{CDM}}h^2)_{\text{min}} \leq \Omega_\chi h^2 \leq (\Omega_{\text{CDM}}h^2)_{\text{max}}$]. This can be appreciated in Figs. 21 and 22, where $C_{NP}$ is plotted against the neutralino

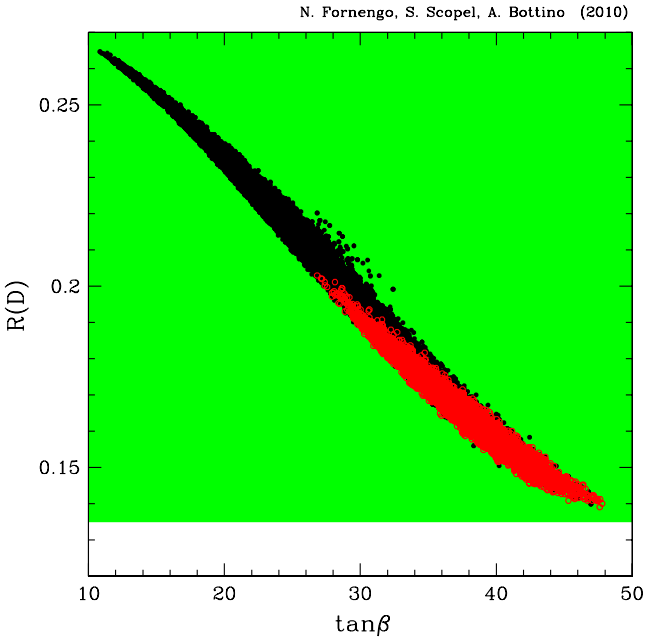


FIG. 18 (color online). Scatter plot of the quantity $R(D)$, calculated according to Eq. (9) of Ref. [76] as a function of $\tan\beta$ in the LNM-$\mathcal{A}$ scan. Black points stand for $m_\chi > 10$ GeV, while the red circles for $m_\chi \leq 10$ GeV. The green horizontal band represents the bottom part of the range of Eq. (42).

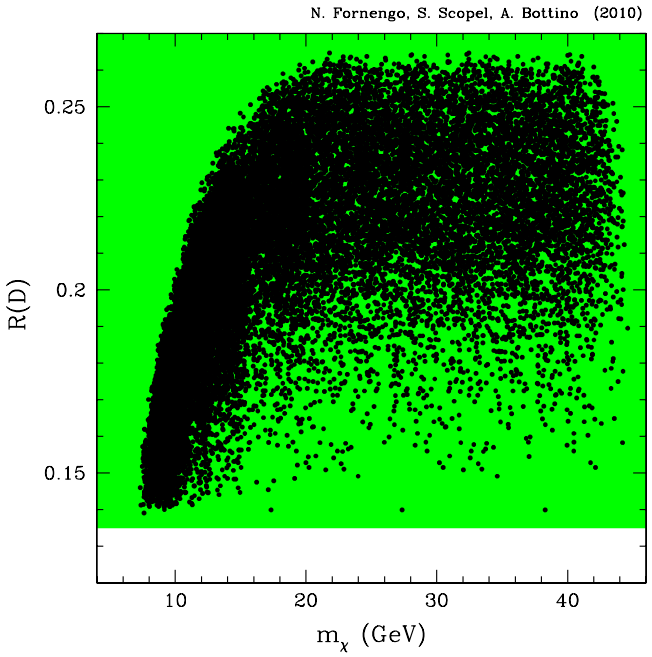


FIG. 19 (color online). Scatter plot of the quantity $R(D)$, calculated according to Eq. (9) of Ref. [76] as a function of $m_\chi$ in the LNM-$\mathcal{A}$ scan. The green horizontal band represents the bottom part of the range of Eq. (42).

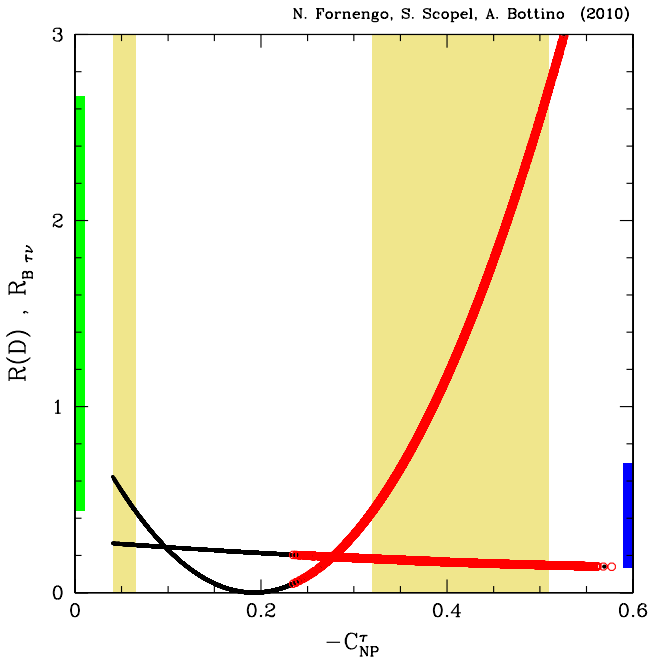


FIG. 20 (color online). $R_{B\tau\nu}$ and $R(D)$ as functions of $C^\tau_{NP}$, for configurations of the LNM-$\mathcal{A}$ scan. The curve with the parabolic shape and the almost straight line represent the values of $R_{B\tau\nu}$ and $R(D)$, respectively, for light neutralinos. The red points denote the neutralino configurations with $m_\chi \leq 10$ GeV. The two ranges along the vertical axes denote the interval of Eq. (41) for $R_{B\tau\nu}$ (in green, on the left) and the interval of Eq. (42) for $R(D)$ (in blue, on the right). The two vertical bands in yellow denote the ranges of $C^\tau_{NP}$ where the experimental intervals of $R_{B\tau\nu}$ and $R(D)$ have a common solution.

mass (Fig. 21) or $\tan\beta$ (Fig. 22). In Fig. 21 the points denoted by red crosses refer to cosmologically dominant neutralinos, and they are compatible with the preferred ranges of $C_{NP}$ for neutralino masses below 13 GeV (and large $\tan\beta$) and in the interval 18–25 GeV (and low $\tan\beta$). In Fig. 22 the red circles refer to configurations with $m_\chi \leq$ 10 GeV. Notice that if we take at face value the current bounds on the $B \to \tau$ decays, light neutralinos would actually be favored.

Nevertheless, we recall that, for the reasons mentioned at the beginning of the present section, it seems premature to enforce these constraints rigidly at the present time (see Ref. [69] for similar comments).

We can conclude the present section on constraints on supersymmetric parameters from the Tevatron collider and the $B$ factories with the following remarks: (i) the upper bound on the branching ratio for the decay $B_s \to \mu^+ + \mu^-$ determined at the Tevatron has a mild effect in constraining the LNM, at variance with what occurs in SUGRA models, (ii) the bounds which are derived from the Higgs bosons searches at the Tevatron do not modify the previously mentioned lower bound $m_\chi \gtrsim 7.5$ GeV, (iii) the measurements of the rare $B$-meson decays at $B$ factories have still to be taken with much caution: combining the present data on $B \to \tau + \nu$ and $B \to D + \tau + \nu$ one derives a range of $\tan\beta/(m_{H^\pm}/120\ \text{GeV})$ which at present might only have some effect on the light-neutralino population for $m_\chi \simeq$ 15–20 GeV, without modifying the lower bound on the neutralino mass.

We finally note that the strict bounds obtained in Ref. [16] on the WIMP-nucleon scattering cross section are mainly due to (a) the use of constraints on $\tan\beta$ derived from D0 Collaboration [79] and CDF [62] data which were subsequently superseded (and relaxed) by Refs. [37,39], respectively; (b) the implementation of bounds restrictively derived from $B$-meson decays data which suffer from sizable uncertainties and which have been in part superseded by the more recent measurements quoted above.

## VII. CONFRONTING RESULTS FROM EXPERIMENTS OF DIRECT DETECTION OF DM PARTICLES

As mentioned in Sec. V, the neutralino interacts mainly by a coherent process with the target nuclei, thus the neutralino-nucleus cross section is conveniently expressed in terms of the neutralino-nucleon cross section $\sigma^{(\text{nucleon})}_{\text{scalar}}$ and then the relevant quantity to be considered is this cross section multiplied by the rescaling factor $\xi$ defined in Sec. V: $\xi\sigma^{(\text{nucleon})}_{\text{scalar}}$.

In Fig. 23 we show the scatter plot representing the supersymmetric configurations of LNM $A$ and subjected to the constraints discussed in Secs. II and IV. The cross